Available online www.ejaet.com

European Journal of Advances in Engineering and Technology, 2024, 11(9):10-22

Research Article ISSN: 2394 - 658X

Finite Element Analysis of Tensile Strength Characteristics of Certain Composite Material Systems with Induced Fiber Waviness

Sai Bhargav Pottavathri[1], Rajeev Nair[2], Ramazan Asmatulu[3]

[1,2,3]Mechanical Engineering Department, Wichita State University, Wichita, Kansas, USA-67226
[2]rajeev.nair@wichita.edu

ABSTRACT

The purpose of this study was to investigate the strength and effectiveness when induced with 'in-plane fiber tow waviness' in carbon, glass and kevlar fibers with thermosetting epoxy systems. An investigation of a single composite ply of carbon/epoxy, AS4/3501-6, IM7-977-3, glass/epoxy and Kevlar/epoxy was carried out to study the effect of fiber tow waviness. Waviness is usually induced by infusion processes and inherent in fabric architectures. Composite structural details like ply drops and ply joints can cause serious fiber misalignment. These are usually dependent on parameters such as ply thickness and have been the subject of recent studies. Waviness is expected to reduce compressive strength due to two primary factors. The fibers may be misoriented, which causes buckling mode of failure in compression and other modes of failure in tension. The waviness leads to an angular shift in the fiber orientation which eventually results in matrix dominated failure on normally orientated ply which is in the primary load direction (00). Maximum stress at failure and maximum load at failure values generated by the finite element model was validated using classic lamination plate theory. A precise geometry of waviness in different materials plies was modeled with different wave severity factor and a parametric study was conducted. Three different defects were modeled: an angle of misalignment ranging from 5 to 15 degrees, a wavelength ranging between 1 to 1.5 inch, and amplitude ranging from 0.05 to 0.1 inch. Load carrying capability of carbon, glass and Kevlar ply dropped drastically with the increase in the severity factor of the defects. This revealed that the effect of 'in-plane fiber tow waviness can lead to poor performance with high stresses that lead to a decrease in the strength ratio, ultimately leading to delaminations and cohesive matrix failure.

Keywords: Composites, in-plane fiber waviness, finite element analysis, abaqus, lamina, tow, ply, misalignment, resin, stress distribution, volume fraction, traction load, strength ratio, shocklam

---

INTRODUCTION

Composite materials are commonly used in aerospace structures until recently. Today these materials are also used widely in other fields such as automotive and energy sectors including in the manufacture of turbine blades.

Clay and Knoth conducted an extensive experimental study in obtaining the capabilities of nine different composite progressive damage analysis methods. These laminates are tested in quasi-static tension and compression to predict the failure and strength of the composite laminates. Unnotched and open-hole coupon tests were conducted to predict the type of damage, location, amount and strength. They also recommended some alternative experimental approaches [1]. Dalgarno et al., analyzed the progressive failure response of the Unnotched and open hole test coupons both in tension and compression using Autodesk's Helius PFA. Their calibrated simulations validate the actual test results conducted on different laminates however simulation results on soft laminates were over predicted because the modeling methods didn't consider explicitly on delaminations [2]. Godines et al., provided a theoretical prediction for damage development for a set of laminated composites using a commercial code GENOA. Unnotched and open-hole configurations are tested in this study. A consistent building block approach which has a multi-scale progressive failure analysis in GENOA were effectively utilized [3]. The importance of the mesh convergence before conducting any failure predictions was investigated by Naghipour and team. This study demonstrated the importance of refining the mesh in in-plane directions for the improved results. Finally, this study

highly recommends employing 2D continuum shell elements whenever possible especially while conducting micromechanics-based analysis [4]. Yuan and Crouch along with Wollschlager, Shojaei and Fish analyzed the performance of 'Altair Multiscale Design' software in the analysis of advance composites aircraft structures. They validated the results of notched and unnotched composite coupons with this software and found that the software validation was very close to the actual observed results [5]. Manufacturing of composite materials is a difficult task especially with respect to maintaining the quality standards. There are many defects induced during the process of manufacturing of composite panels. Most of the defects are due to mismatch of coefficient of thermal expansion, improper fiber volume fraction, void contents, interfacial de-bonding, un-wetted fibers, fiber misalignments or fiber waviness in composite panels [6]. Most of the defects are due to mismatch of coefficient of thermal expansion, improper fiber volume fraction, void contents, fiber misalignments or fiber waviness. For quite some time now, researchers have been trying to improve the manufacturing systems that can aid in the processing of efficient composite materials [7]. Several engineering applications and improvements evolved in these efforts and helped in better usage, new advanced materials, and high precision manufacturing processes of composite materials [8-10].

For minimal fuel consumption and weight reduction, every airplane manufacturer utilizes composites with varying percentages. There is a huge gain in achieving tailored properties by using composites and therefore manufacturing a defect-free composite is becoming a challenging task. There are major defects like delamination, porosity, resin rich areas, cracks and voids which still cause concern [11]. Bundle of fibers combined together is called a tow. Tow waviness can be unintentionally induced in a uni-directional dry carbon ply during the manufacturing process. This unintentionally induced waviness can be categorized into two types. The first one is in-plane waviness and the second one is out-plane waviness. In-plane waviness is a kind of fiber tow waviness which is induced within the lamina, where the fiber direction deviates from 0º to higher angles at a particular location or throughout the lamina. The out of plane waviness is a kind of waviness which is induced through the plies in the thickness direction. In this paper, the primary focus is on the in-plane tow waviness and their severity in reducing the overall mechanical strength of the composites.

In-plane fiber waviness can be categorized mainly into two types, one is normal waviness which carries the wave pattern through the lamina. This could occur due to poor binder failure along the width of the lamina. The other type of in-plane waviness is called localized waviness. Here the tow will not only be misaligned to their preferred direction but also create resin rich packets which lead to uneven volume fraction in a composite structure. These are highly sensitive to external loads and creates high stress near the resin rich areas. The properties of the composite materials depend on the material properties which are used to make composite laminates and the distribution of the materials. The most important properties of the composite materials are its mechanical properties. The materials that are selected to make a composite panel should satisfy the application that usually requires strength, shape, and rigidity [12, 13]. The mechanical properties of the composites can be predicted using the rule of mixture, although the rule of mixtures has not been used successfully in major aerospace programs for predicting properties other than fiber dominated moduli. Rosen [14] predicted compressive strength of the laminate during micro-buckling. The author considered the kinking and buckling condition of the fibers inside the laminate and predicted the strength of the composite laminate during compression. Hsiao and Daniel [15] studied the effect of fiber waviness on stiffness and strength reduction in unidirectional composites under compressive loading conditions. This research primarily focused on the modeling of fiber waviness patterns that are generally found in the laminates. Garnich and Karami [16] investigated the fiber waviness in the composite panel using a computational method. They considered the micromechanical model of fiber and matrix unit cell. The effect of stress in the wavy laminate was studied by considering several failure predictions. The stress distribution and its effects in the wavy laminate during axial loading and fiber waviness influence on the predictions for the failure were also studied. Lei [17] identified the effects of in-plane fiber waviness on the static and fatigue strength of fiberglass composites. They investigated the fiber failure and delaminations in a composite material when induced with in-plane waviness during tensile loading. From this study, it was concluded that in-plane waviness causes a drastic strength reduction. As the severity of waviness increases, there is a greater dropdown in the mechanical strength of the composites.

Chun et al. [18] investigated the response of laminated composites during tension and compression. They focused on the graded, uniform and local fiber waviness patterns which are found commonly in laminates. Young's modulus along the longitudinal direction was found to be reduced, as shown by their analytical model. It was also shown that the strength of the laminate gets influenced by the degree of fiber waviness, wavy fibers getting softened by the compressive loads and getting stiffer by the tensile loads. A recent study conducted by Joyce and Moon [19] focused on the effect of in-plane fiber waviness in the strength reduction. They found that due to fiber waviness, there is significant strength reduction and subsequent failure of the composite laminates due to stress concentration factors that are developed near the tabbed region. Kugler and Moon [20] found that fiber waviness was primarily caused by the manufacturing and processing methods. They investigated the processing parameters such as the temperature at which the composite gets cured, the time duration of the curing process of composite laminates and external pressure that is applied on the surface of the composite during the curing process. The rate of sudden cooling the composite laminate and the tool plate material (which is used to lay up the composite undergoes after

curing) undergoes, also leads to fiber waviness. The mismatch of the thermal coefficient between the tool plate and the laminate composite was found to be one of the potential reasons for fiber waviness.

Bogetti and Gillespie [21, 22] developed an analytical model in order to predict the effects of fiber waviness in a cross-ply laminate. The model was developed to predict the effect of waviness in the strength reduction and stiffness in a composite laminate. The basis of their study was to evaluate the structural response of a cylindrical composite that is made with cross-ply laminates during its construction. Martinez [23] studied the effects of misalignments in a fiber on the compression strength of composites using glass/polyester laminate specimen. Misalignment of the fiber was introduced by twisting the fiber tows at a certain amount before the impregnation of the resin. It showed a reduction in the compressive strength with a misalignment angle which is greater than 10º for both carbon and glass fibers. Mrse and Piggott [24] studied the effect of intentional and unintentional misalignments of the fiber on the compressive properties of unidirectional laminates. They considered unidirectional carbon fiber laminate for their study. Here, unidirectional carbon fibers are made with AS4 carbon and reinforced with polyether ether ketone (PEEK) prepreg which was crimped to various degrees to change the waviness in the fiber. A microscope was used to measure the wavelength and amplitude of the misaligned fibers, and compressive strength and compressive modulus are correlated. Mandell and Samborsky [25, 26] conducted research on fabric weave composite structures and found that the compressive strength of the composite reduced because of the through-thickness waviness of the fibers and the high tensile strength of the laminate. Harris and Lee [27] developed a micromechanical model of laminates induced with fiber waviness and studied its strength and stiffness characteristics, and found that waviness had a deteriorating effect on such properties. Poe et al. [28, 29] conducted tensile strength analysis on a thick composite material (filament wound, carbon fiber solid rocket case of a motor) that experienced a low-velocity impact. They investigated the tensile strength of the damaged composite panel and found that it lead to a reduction of 39 % strength reduction than the expected value. It was concluded that the strength of the composite laminate got reduced due to fiber waviness in one of the plies, which was induced unintentionally during the manufacturing process. Kar et al. [30] studied fractographic and microstructural properties of composites that undergo compression. Their research showed that the resin rich areas increased the moisture absorption that eventually resulted in the fiber distribution inside the composite becoming uneven, ultimately weakening the properties of the composite material. The authors of this paper have done some prior work on examining the effect of in-plane fiber tow waviness on the tensile strength properties of fiber reinforced composites of carbon/epoxy AS4/3501-6. Waviness was found to substantially reduce the strength characteristics of the carbon/epoxy material [31].

EXPERIMENTAL

Modeling

The composite single ply is built using the finite element analysis software Abaqus® (Abaqus version 6.14 was used in this study). The composite lamina is a combination of a bunch of tows which are grouped together using binder threads. Tow is defined as a bunch of untwisted fiber filaments. The composite lamina is made out of combining the tows together, which includes a resin that is impregnated with a predefined volume fraction in each of the carbon, glass, Kevlar fibers. Fourteen tows are combined together to form a composite lamina, where the width and thickness of the each tow are 0.07 inches (0.001778 m) and 0.0078 inches (0.000198 m). The total width of the lamina is 0.98 inches (0.025 m). Resin rich location is created by misaligning one of the following tows. The location of the resin rich area is modeled so that it is at the center of the composite lamina. Fiber waviness is assumed to be followed by the corresponding tows and depending on the angle of the wave, the corresponding wavy tows get terminated along the width of the lamina. Since the concern in this study is about a single lamina, there will be no coupling between the components, i.e. $[B_{ij}] = 0$. Since a uniaxial tension load is applied on the lamina, no bending and twisting moments apply in this case.

Hence the above matrix gets reduced.

$$[N]=[A]\left[\varepsilon^0_{xy}\right] \quad (1)$$

Where, N = Forces per Unit Length, A= Extensional Stiffness Matrix, ε^0_{xy}= Midplane Strains.

The In-plane stiffness matrix [A] for entire laminate can be expanded as below.

$$\begin{bmatrix} Nx \\ Ny \\ Ns \end{bmatrix} = \begin{bmatrix} A_{xx} & A_{xy} & A_{xs} \\ A_{xy} & A_{yy} & A_{ys} \\ A_{xs} & A_{ys} & A_{ss} \end{bmatrix} \begin{bmatrix} \varepsilon^0_x \\ \varepsilon^0_y \\ \gamma^0_s \end{bmatrix} \quad (2)$$

$$N_x = (N_x)_1 + (N_x)_2 + (N_x)_3 + \ldots + (N_x) \quad (3)$$

$$N_x = (\sigma_x)_1(h_1-h_0) + (\sigma_x)_2(h_2-h_1) + (\sigma_x)_3(h_3-h_2) + \ldots\ldots\ldots\ldots + (\sigma_x)_n (h_n-h_{n-1}) \quad (4)$$

Where, h_1 = Distance between midplane and top surface of the bottom ply, h_0= Distance between midplane and bottom surface of the bottom ply, $h_1-h_0 = t_1$ = Thickness of ply 1, t_k= Thickness of Kth ply.

$$N_x = \sum_{k=1}^{n} t_k \quad [Q_{xx} \quad Q_{xy} \quad Q_{xs}]_k \begin{bmatrix} \varepsilon_x^o \\ \varepsilon_y^o \\ \gamma_s^o \end{bmatrix} \quad (5)$$

Where, $Q_{xx} = Q_{xy} = Q_{xs}$= Stifness Matrix.

$\varepsilon_x^o = \varepsilon_y^o = \gamma_s^o$=Mid plane Strains, t_k = Thickness of Kth ply.

Similarly,

$$N_y = \sum_{k=1}^{n} t_k \quad [Q_{xy} \quad Q_{yy} \quad Q_{ys}]_k \begin{bmatrix} \varepsilon_x^o \\ \varepsilon_y^o \\ \gamma_s^o \end{bmatrix} \quad (6)$$

$$N_s = \sum_{k=1}^{n} t_k \quad [Q_{xs} \quad Q_{ys} \quad Q_{ss}]_k \begin{bmatrix} \varepsilon_x^o \\ \varepsilon_y^o \\ \gamma_s^o \end{bmatrix} \quad (7)$$

The above three in-plane forces can be combined as follows.

$$\begin{bmatrix} N_x \\ N_x \\ N_s \end{bmatrix} = \sum_{k=1}^{n} \begin{bmatrix} Q_{xx} & Q_{xy} & Q_{xs} \\ Q_{xy} & Q_{yy} & Q_{ys} \\ Q_{xs} & Q_{ys} & Q_{ss} \end{bmatrix}_k \begin{bmatrix} \varepsilon_x^o \\ \varepsilon_y^o \\ \gamma_s^o \end{bmatrix} t_k = \begin{bmatrix} A_{xx} & A_{xy} & A_{xs} \\ A_{xy} & A_{yy} & A_{ys} \\ A_{xs} & A_{ys} & A_{ss} \end{bmatrix} \begin{bmatrix} \varepsilon_x^o \\ \varepsilon_y^o \\ \gamma_s^o \end{bmatrix} \quad (8)$$

The main objective of this study is to analyze the effect of fiber waviness and resin rich areas in the strength of the single lamina using Finite Element Analysis (FEA). The research focus is to analyze the magnitude and stress concentration in a lamina at the location of the fiber waviness and the resin rich areas. Mechanics of materials equations described above were used to find out the maximum failure stress. Experimental results conducted by Hsiao and Daniel 15 were validated using Shocklam® (a software developed by Dr. K.S. Raju, Professor of Aerospace Department at Wichita State University, that uses mechanics equations related to composites for stress analysis) [31, 32] and Abaqus® finite element formulation results. Attempts were made to fabricate the laminate (defective and non-defective) in a wet layup process to also validate the results experimentally. It was found that for defective laminates, an exact waviness pattern created experimentally before the wet-layup process usually changed after the wet-layup process was completed because of obvious external factors involved. In addition, a manual wet-layup process and a study of the tensile strength, regarding studying waviness had an inherent problem in repeatability due to different variables including porosity, uneven binder spread etc., that resulted in skewed results.

PROCEDURE

A comparative FEA analysis was done to study the three types of defects which are minor, major and severe. The analysis was carried out on a carbon/epoxy material AS4/3501-6, IM7/977-3, glass/epoxy, Kevlar/epoxy. A three-dimensional finite element model was built using Abaqus®. Linear static analysis approach is used in this study. Maximum stress failure criteria is considered in evaluating the stresses in the defects. The purpose of this study is to predict the load carrying capabilities of the different composite laminas when induced with fiber waviness and resin rich areas combined. The failure stresses are predicted using Abaqus. Depending on the severity of the defects the lamina (mechanical properties given in table 1) reaches its failure stress accordingly and the load carrying capacity also gets reduced. Stress values of the model without any waviness are validated using classical lamination plate theory approach.

The finite element model was built by modeling 14 tows (a bunch of fibers) individually which are assembled together using tie constraints. A tie constraint ties the two surfaces of the fiber tows together and does not allow any relative motion between them [33]. The length and width of each tow are 9.84 inches (0.25 m) and 0.07 inch (0.001778 m) respectively. These 14 tows are assembled together to create a single lamina and a material orientation for each tow is assigned as shown in Figure 1. One end of the composite lamina is fixed in all degrees of freedom while a longitudinal tensile load is applied on the other end.

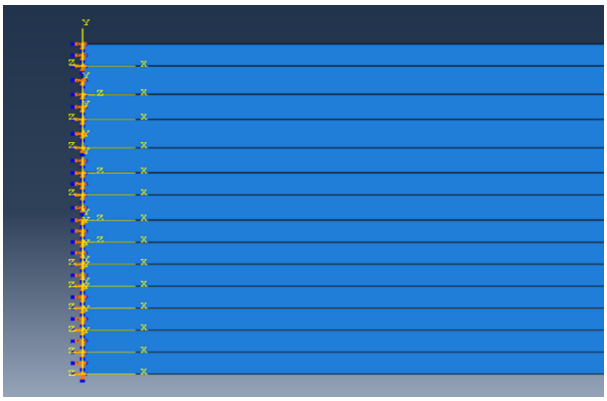

Figure 1: Lamina modeling in Abaqus (total width – 0.98 inch (0.025 m)).

Table 1: Mechanical Properties of Laminas. [34, 35]

Property	**Carbon /Epoxy (AS4/3501-6)**	**Carbon /Epoxy (IM7/977-3)**	**Glass/Epoxy**	**Kevlar/Epoxy (Aramid 49)**
Volume Fraction (V_f)	0.63	0.65	0.55	0.60
Density (lb/in^3)	0.058	0.058	0.071	0.050
E_1(Msi)	21.3	27.7	6.0	11.6
E_2(Msi)	1.50	1.44	1.50	0.80
G_{12}(Msi)	1.00	1.13	0.62	0.31
υ_{12}	0.27	0.35	0.28	0.34
Major Poisson ratio				
υ_{21}	0.02	0.02	0.06	0.02
Minor Poisson ratio				
F_{1t} (ksi)	330	470	165	205
Longitudinal Tensile strength				
F_{2t} (ksi)	8.3	8.9	5.7	4.2
Transverse Tensile strength				
F_6 (ksi)	11.0	10.9	12.9	7.1
In-plane Shear Strength				

Table 2: Wave parameter value for the lamina.

Defect	**Wavelength, Inch (m)**	**Amplitude, Inch (m)**	**Angle (degrees)**
Minor	1 (0.0254)	0.03 (0.0007)	5
Major	1.25 (0.0317)	0.05 (0.0012)	10
Severe	1.50 (0.0381)	0.07 (0.0017)	15

The waviness of the tow is modeled starting in the 7th tow from the bottom based on values as shown in table 2. Waviness patterns are induced in the rest of the tows in the y-axis and eventually gets terminated at edges as shown in Figure 3. The termination point of the wavy tows is assumed in this analysis because in a real time scenario, fiber tow waviness cannot be exactly symmetrical in geometry and it depends on the type of fiber, weave architecture, and density of the fiber tows which are combined together with binders. To simplify the analysis, the termination point of waviness will increase along with an increase in the angle of the waviness. As per this assumption, the more the angle of misalignment, it would require correspondingly more successive fiber tows to reach the waviness termination point to become straight tows. The linear implicit static analysis is used in this finite element analysis and 3D 8 node brick elements are used to represent the elements. A fine mesh size of 0.000254 m is maintained throughout the analysis for efficient results.

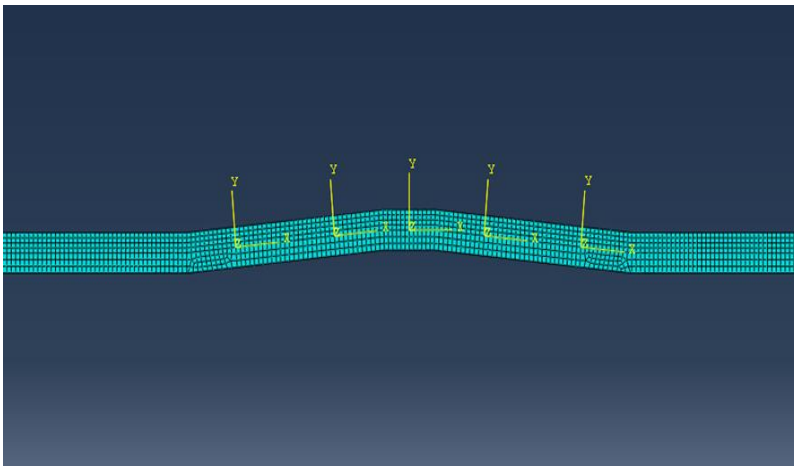

Figure 2: Material orientation of the single tow (width – 0.07 inch (0.001778 m)).

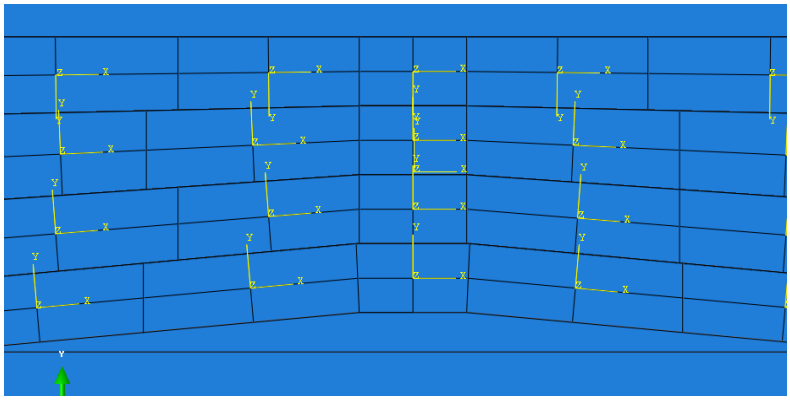

Figure 3: Resin rich area and assembly of wavy tows of the minor defect.

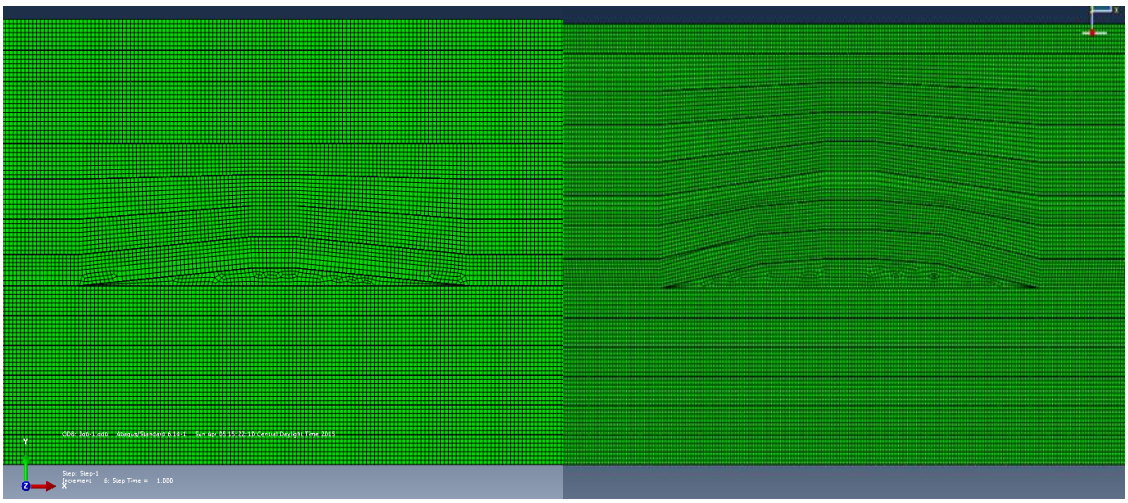

Figure 4: (a) Minor defect of 1" (0.025 m) wavelength, (b) Major defect -1.25" (0.031m) wavelength.

Since the fiber tows get misaligned, the material orientation of the fiber tow changes accordingly with the direction of the fibers. So the misaligned tow is discretized into different sections to assign material orientation, creating a local coordinate system of the misaligned fiber tows as shown in figure 2. Similarly, material orientation is assigned to all tows and assembled together using tie constraints. The misaligned portion is then filled with resin and acts as a resin rich area as shown in figure 3. The three defects that are modeled are shown in detail in figures 4 and 5.

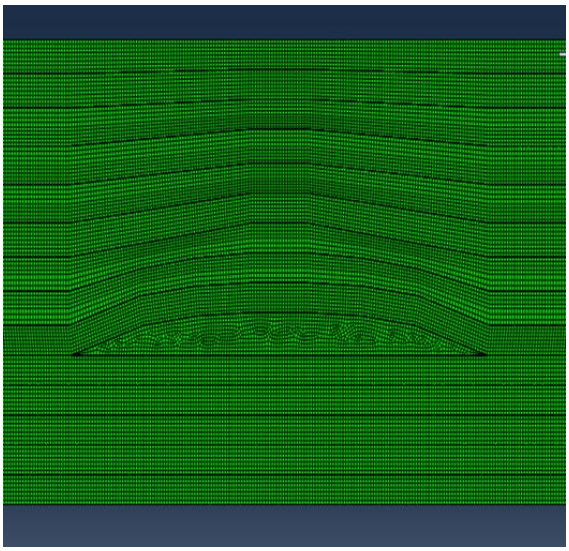

Figure 5: Severe defect with 1.50" (0.0381 m) wavelength.

RESULTS

Load vs. Stress Analysis

Mechanics of material equations (Shocklam® [32]) were used to find approximate values of the maximum load that the (AS4/3501-6), (IM7/977-3), (glass/epoxy), (Kevlar/epoxy) plain lamina could carry to reach the maximum stress values, and these values were validated using Abaqus. A surface traction force is applied on one end of the lamina model. This load is the maximum load that the lamina can resist before it reaches the failure stress value. It is seen that the load carrying capacity gets gradually reduced in these three defects. The reduction in load carrying capacity for AS4/3501-6, IM7/977-3, glass/epoxy, Kevlar/epoxy is shown in figures 6, 7, 8 and 9. The composite lamina with defects results in high stresses. In this analysis, the materials experienced a maximum load which results in maximum failure. It can also be hypothesized that as the severity of the defect increases, there is an obvious decrease in the load carrying capacity of the different material laminas.

As we can observe in Figure 6, the material with no defect resisted the load of 2418 lb/in (traction load 310000 lb/in^2) during the maximum stress limit. The model with minor defect experienced the maximum value of stress when it reached reduced load of 2106 lb/in (traction load 270000 lb/in^2) which reduced the load carrying capacity to 13 %. Model with major defect experienced the maximum value of stress when it reached reduced load of 2028 lb/in (traction load 260000 lb/in^2) which reduced the load carrying capacity to 16%, and the model with severe defect reached reduced load drastically 1755 lb/in (traction load 225000 lb/in^2) which reduced the load carrying capacity to 27 %. These percentages are high because there are no other plies surrounding to it to transfer the load.

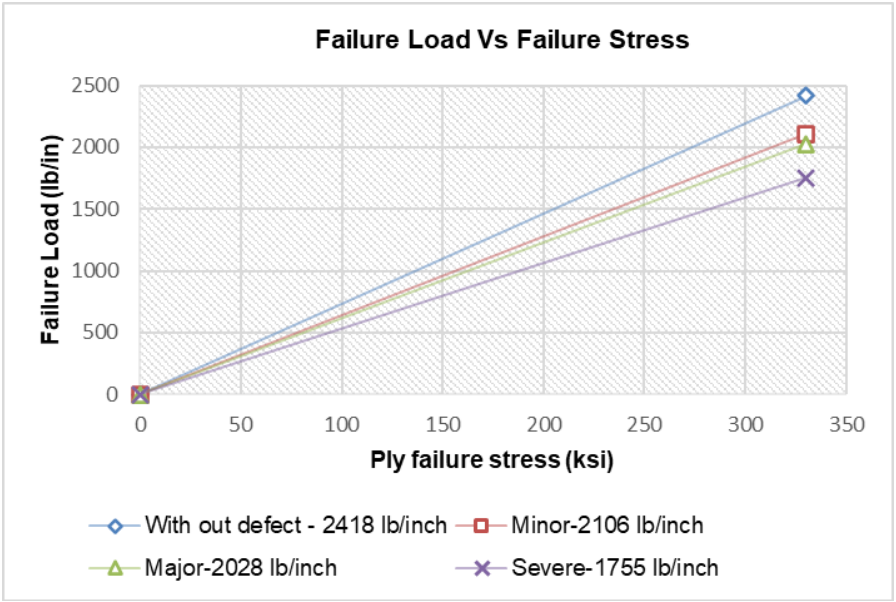

Figure 6: Reduction in the load carrying capacity of AS4/3501-6.

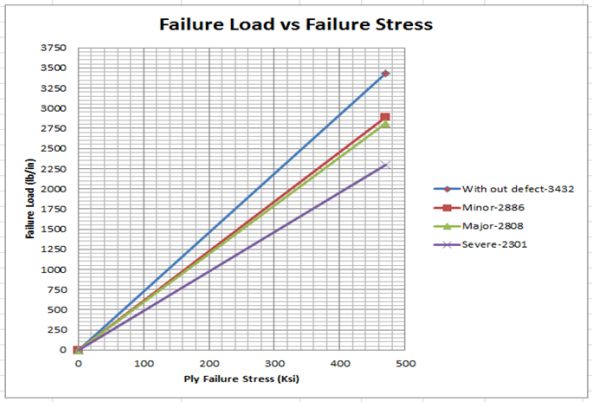

Figure 7: Reduction in the load carrying capacity of IM7/977-3.

As seen in Figure 7, the material with no defect resisted the load of 3432 lb/in (traction load 440000 lb/in^2) during the maximum stress limit, the model with minor defect experienced the maximum value of stress when it reached the reduced load of 2886 lb/in (370000 lb/in^2) which reduced the load carrying capacity to 16%. The model with major defect experienced the maximum value of stress when it reached the reduced load of 2808 lb/in (360000 lb/in^2) which reduced the load carrying capacity to 17%, and the model with severe defect reached the reduced load drastically 2301 lb/in (295000 lb/in^2) which reduced the load carrying capacity to 33%. These percentages are considerably high because there are no other plies surrounding it to transfer the load except the resin.

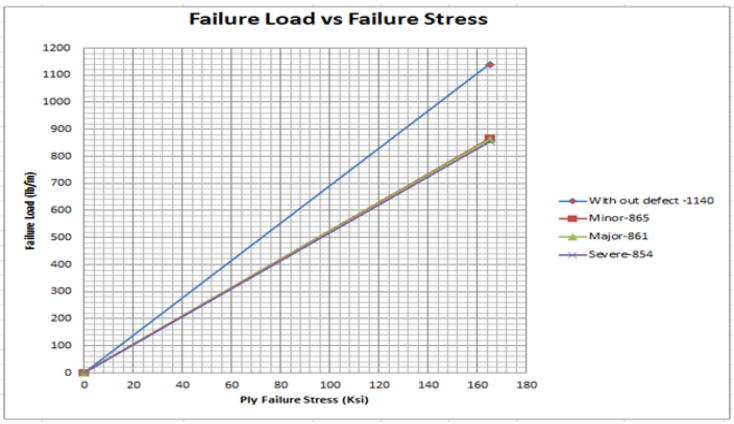

Figure 8: Reduction in the load carrying capacity of glass/epoxy.

The load carrying capacity of the glass/epoxy with minor, major and severe defect is reduced from 1140 lb/in (surface traction of 146100 lb/in^2) to 865.8 ksi (111000 lb/in^2) for minor defect, to 861 ksi (110500 lb/in^2) for major defect and to 854 ksi (109500 lb/in^2) for severe defect. The load carrying capacity of the lamina drastically reduces to 24 % for the minor defect, 24.5% for the major defect, and 25% for the severe defect.

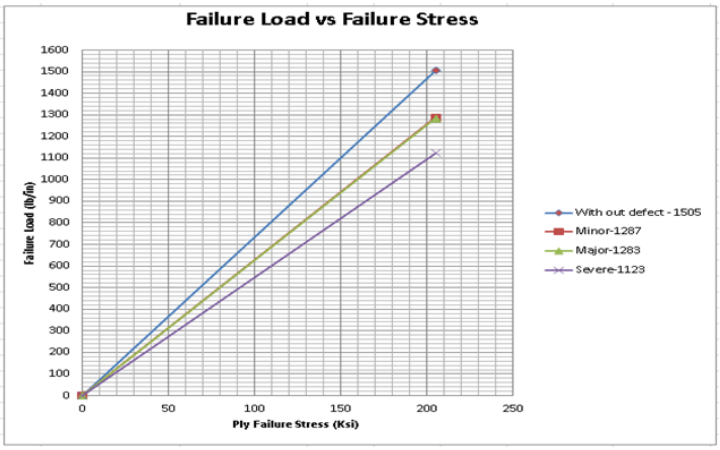

Figure 9: Reduction in the load carrying capacity of Kevlar/epoxy.

In Figure 9, the material with no defect resisted the load of 1505 lb/in (traction load 193000 lb/in^2) during the maximum stress limit, the model with minor defect experienced the maximum value of stress when it reached the reduced load of 1287 lb/in (traction load 165000 lb/in^2) that hence reduced the load carrying capacity to 14%, model with major defect experienced the maximum value of stress when it reached reduced load of 1283lb/in (traction load 164500 lb/in^2) that hence reduced the load carrying capacity to 15%. Both the minor and major defects exhibited the same level of stresses. The Kevlar/epoxy material fails on same predicted load for the major and minor defect geometry. The model with severe defect reached the reduced load drastically at 1123 lb/in (traction load 144000 lb/in^2) that reduced the load carrying capacity to 26%. These percentages are noticeably high because there are no other plies surrounding it to transfer the load. A 1000 lb/in (175126 N/m)-(128205 lb/in^2 (884 Mpa)) load is applied on one side of the four models (one without defect plies and the rest defective models) on AS4/3501-6, IM7-977-3, Kevlar/epoxy material. An 800lb/in the load is applied on glass/epoxy. Due to the resin rich area and the uneven distribution of volume fraction in the lamina, stress concentrations are developed at the weakest point where the failure may take place. The stress values get increased near the vicinity of the defect at the same loading conditions for the three different defects for all the materials.

COMPARISON

Table 3 compares the stresses and the percentage increase in stress for four material types and the four cases of no defect/defect models. It can be seen that the percentage increase in stress follows an upward climb as the case history moves from 'no defect' to 'severe defect.'

Table 3. Stress values and percentage increase with an applied load of 1000 lb/in (175126 N/m).

Cases	**Defect # - AS4/3501-6**	**Stress in ksi (Mpa)**	**% Increase in stress**
No Defect	0	137 (945)	0
Minor	1	158 (1089)	13
Major	2	162 (1117)	15
Severe	3	187 (1289)	27
Cases	**Defect # - IM7/977-3**	**Stress in ksi (MPa)**	**% Increase in stress**
No Defect	0	138(951)	0
Minor	1	163 (1123)	15
Major	2	167 (1151)	17
Severe	3	204 (1406)	32
Cases	**Defect # - Glass/Epoxy**	**Stress in ksi (MPa)**	**% Increase in stress**
No Defect	0	155(1068)	0
Minor	1	153 (1054)	25
Major	2	153.5 (1058)	25
Severe	3	154.7 (1066)	26
Cases	**Defect # - Kevlar/Epoxy**	**Stress in ksi (MPa)**	**% Increase in stress**
No Defect	0	136(937)	0
Minor	1	159 (1096)	14
Major	2	160 (1103)	15
Severe	3	184 (1268)	26

DISCUSSION

Discussion of Stress Distribution in the Vicinity of the AS4/3501-6 Defects

A brief discussion on the stress distribution near the defective zones for AS4/3501-6 is outlined below. It is observed that the load carrying capacity gets reduced as the severity of the defect increases. Accordingly, stress distribution of these three defects varies depending on the architecture of the defect. A Von Mises stress display of the results is taken when the model gets maximum stress values with the reduced loading condition. Figure 10 illustrates the stress values in the vicinity of the defects. In Figure 11, the x-axis represents the width of the model while the y-axis represents the stress values at the each nodal points. Similarly Figures 12 and 13 represents the high-stress distribution around the vicinity of major and severe defects. It can be clearly seen that the stress distribution pattern shows an enhanced spread along the positive y-axis (where the waviness exists) clearly articulating the effect of waviness. In the negative y-axis, a much smaller stress distribution can be seen although no waviness was modeled on that side. Poisson's effects are visible here and it is hypothesized that the resin-rich areas in the middle quickly erode the structural cohesiveness of the lamina in the negative transverse direction and as a direct result, substantially reduces its load-carrying capacity. Similar effects are observed in IM7/9773, Kevlar/Epoxy and glass/epoxy with some variations.

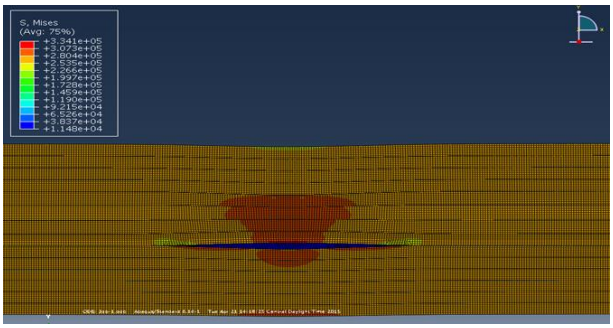

Figure 10: Stress (psi) distributions near the vicinity of the minor defect.

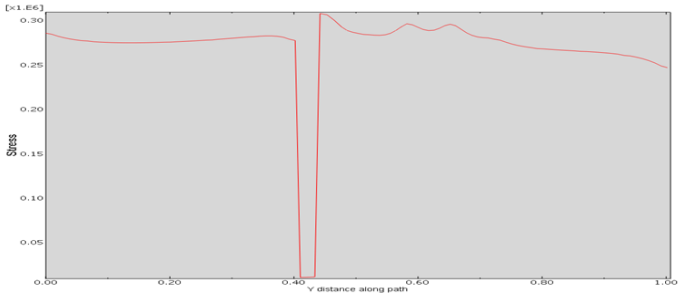

Figure 11: Stress distributions along the width of the minor defect (stress in psi, y-distance in inches).

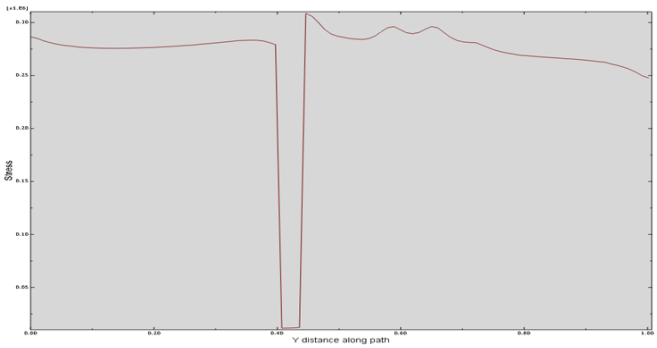

Figure 12. *Stress distributions along the width of the major defect (stress in psi, y-distance in inches).*

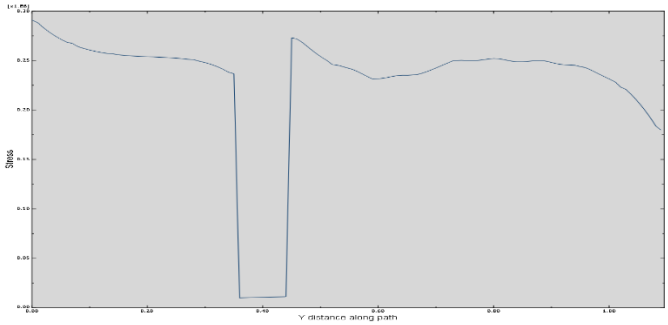

Figure 13: Stress distributions along the width of the severe defect (stress in psi, y-distance in inches).

CONCLUSIONS

The effect of in-plane fiber waviness is studied by modeling laminas and analyzing both in-plane fiber tow waviness and resin rich pockets using finite element tool, Abaqus. It concludes that the effect of the defect in a lamina will depend on the properties of the material and as the severity of the defect increases the load carrying capacity of both the lamina and laminate reduces. A brief summary of the major findings in this study is provided below.

S4/3501-6

- The effect of major, minor, and severe fiber waviness and the resin rich area were analyzed in a lamina made with AS4/3501-6

- The load carrying capacity of the single lamina got reduced 13% for a minor defect. 15% for major defect and 27% of the severe defect.
- High-stress concentrations are developed near the vicinity of the defect, the stresses are increased from 137 ksi to 187 ksi at an application of fixed load 1000ksi on the three laminas,
- The strength ratio of the lamina got reduced from 2.42 (no defect) to 1.78 (severe defect) at an applied load of 1000 lb/in
- Strain values got increased to 40 % as the severity of the defect increases at the failure loads of the lamina.

IM7/977-3

- The effect of major, minor, and severe fiber waviness and the resin rich area were analyzed in a lamina made with IM7977-3
- The load carrying capacity of the single lamina got reduced 15% for a minor defect. 17% for major defect and 32% of the severe defect.
- High-stress concentrations are developed near the vicinity of the defect; the stresses are increased from 138 ksi to 204 ksi at an application of fixed load 1000ksi on the three laminas.
- The strength ratio of the lamina got reduced from 3.41 (no defect) to 2.30(severe defect) at an applied load of 1000 lb/in
- Strain values got increased to 45 % as the severity of the defect increases at the failure loads of the lamina.

Glass/Epoxy

- The effect of major, minor, and severe fiber waviness and the resin rich area were analyzed in a lamina made of glass/epoxy
- The failure was occurring in the boundary conditions, but the uneven stress distributions were developed near the vicinity of the defect.
- The load carrying capacity of the single lamina got reduced 25% for a minor defect. 25% for major defect and 26% of the severe defect.
- High-stress concentrations are developed near the vicinity of the defect, the stresses are increased from 115 ksi to 154 ksi at an application of fixed load 800 lb/in on the three laminas,
- The strength ratio of the lamina got reduced from 1.43 (no defect) to 1.07 (severe defect) at an applied load of 800 lb/in.

Kevlar /Epoxy

- The effect of major, minor, and severe fiber waviness and the resin rich area were analyzed in a lamina made with Kevlar/Epoxy
- The load carrying capacity of the single lamina got reduced 14% for a minor defect. 15% for major defect and 26% of the severe defect.
- High stress concentrations are developed near the vicinity of the defect, the stresses are increased from 136ksi to 184ksi at an application of fixed load 1000ksi on the three laminas.
- The strength ratio of the lamina got reduced from 1.51(no Defect) to 1.11(severe Defect) at an applied load of 1000 lb/in.
- Strain values got increased to 41 % as the severity of the defect increases at the failure loads of the lamina.

ACKNOWLEDGEMENT

The authors gratefully acknowledge the financial and technical support by the College of Engineering at Wichita State University for the present work.

REFERENCES

[1]. Clay SB and Knoth PM. Experimental results of quasi-static testing for calibration and validation of composite progressive damage analysis methods. Journal of Composite Materials 2016; 0: 0021998316658539. DOI: doi:10.1177/0021998316658539.

[2]. Dalgarno RW, Action JE, Robbins DH, et al. Failure simulations of open-hole and unnotched IM7/977-3 coupons subjected to quasi-static loading using Autodesk Helius PFA. Journal of Composite Materials 2016; 0: 0021998316653174. DOI: doi:10.1177/0021998316653174.

[3]. Godines C, DorMohammadi S, Abdi F, et al. Damage tolerant composite design principles for aircraft components under static service loading using multi-scale progressive failure analysis. Journal of Composite Materials 2016; 0: 0021998316671575. DOI: doi:10.1177/0021998316671575.

[4]. Naghipour P, Arnold SM, Pineda EJ, et al. Multiscale static analysis of notched and unnotched laminates using the generalized method of cells. Journal of Composite Materials 2016; 0: 0021998316651708. DOI: doi:10.1177/0021998316651708.

[5]. Yuan Z, Crouch R, Wollschlager J, et al. Assessment of Altair Multiscale Designer for damage tolerant design principles (DTDP) of advanced composite aircraft structures. Journal of Composite Materials 2016; 0: 0021998316651707. DOI: doi:10.1177/0021998316651707.
[6]. Dresselhaus MS, Dresselhaus G and Eklund PC. Chapter 2 - Carbon Materials. Science of Fullerenes and Carbon Nanotubes. San Diego: Academic Press, 1996, pp.15-59.
[7]. Toussaint AF, Luner, P. The Wetting Properties of Hydrophobically Modified Cellulose Surfaces. In: 10th Cellulose Conference New York, 1988, pp.1515-1530. New York.
[8]. Sandler J, Shaffer MSP, Prasse T, et al. Development of a dispersion process for carbon nanotubes in an epoxy matrix and the resulting electrical properties. Polymer 1999; 40: 5967-5971. DOI: http://dx.doi.org/10.1016/S0032-3861(99)00166-4.
[9]. Bower C, Rosen R, Jin L, et al. Deformation of carbon nanotubes in nanotube–polymer composites. Applied Physics Letters 1999; 74: 3317-3319. DOI: 10.1063/1.123330.
[10]. Tibbetts GG and C. P. Beetz J. Mechanical properties of vapour-grown carbon fibres. Journal of Physics D: Applied Physics 1987; 20: 292.
[11]. Das S. Life cycle assessment of carbon fiber-reinforced polymer composites. The International Journal of Life Cycle Assessment 2011; 16: 268-282. journal article. DOI: 10.1007/s11367-011-0264-z.
[12]. Narayanaswami R and Adelman HM. Evaluation of the Tensor Polynomial and Hoffman Strength Theories for Composite Materials. Journal of Composite Materials 1977; 11: 366-377. DOI: doi:10.1177/002199837701100401.
[13]. Eichhorn S, Baillie C, Zafeiropoulos N, et al. Review: current international research into cellulosic fibres and composites. J Mater Sci 2001; 36: 2107-2131.
[14]. Rosen BW. Mechanics of Composite Strengthening. In: Bush SH (ed) Fiber Composite Materials. Metals Park, Ohio: American Society for Metals, 1964, pp.37-75.
[15]. Hsiao HM and Daniel IM. Effect of fiber waviness on stiffness and strength reduction of unidirectional composites under compressive loading. Composites Science and Technology 1996; 56: 581-593. DOI: http://dx.doi.org/10.1016/0266-3538(96)00045-0.
[16]. Garnich MR and Karami G. Localized Fiber Waviness and Implications for Failure in Unidirectional Composites. Journal of Composite Materials 2005; 39: 1225-1245. DOI: doi:10.1177/0021998305048748.
[17]. Wang L. Effects of In-plane Fiber Waviness on the Static and Fatigue Strength of Fiberglass. Montana State University--Bozeman, 2001.
[18]. Chun H-J, Shin J-Y and Daniel IM. Effects of material and geometric nonlinearities on the tensile and compressive behavior of composite materials with fiber waviness. Composites Science and Technology 2001; 61: 125-134. DOI: http://dx.doi.org/10.1016/S0266-3538(00)00201-3.
[19]. Joyce PJ, Kugler D and Moon TJ. A Technique for Characterizing Process-Induced Fiber Waviness in Unidirectional Composite Laminates-Using Optical Microscopy. Journal of Composite Materials 1997; 31: 1694-1727. DOI: doi:10.1177/002199839703101702.
[20]. Kugler D and Moon TJ. Identification of the Most Significant Processing Parameters on the Development of Fiber Waviness in Thin Laminates. Journal of Composite Materials 2002; 36: 1451-1479. DOI: doi:10.1177/0021998302036012575.
[21]. Bogetti TA, John W. Gillespie J and Lamontia MA. Influence of Ply Waviness on the Stiffness and Strength Reduction on Composite Laminates. Journal of Thermoplastic Composite Materials 1992; 5: 344-369. DOI: doi:10.1177/089270579200500405.
[22]. Bogetti TA, John W. Gillespie J and Lamontia MA. The Influence of Ply Waviness with Nonlinear Shear on the Stiffness and Strength Reduction of Composite Laminates. Journal of Thermoplastic Composite Materials 1994; 7: 76-90. DOI: doi:10.1177/089270579400700201.
[23]. Martinez GM, Piggott MR, Bainbridge DMR, et al. The compression strength of composites with kinked, misaligned and poorly adhering fibres. J Mater Sci 1981; 16: 2831-2836. journal article. DOI: 10.1007/bf00552967.
[24]. Mrse AM and Piggott MR. Compressive properties of unidirectional carbon fibre laminates: II. The effects of unintentional and intentional fibre misalignments. Composites Science and Technology 1993; 46: 219-227. DOI: http://dx.doi.org/10.1016/0266-3538(93)90156-B.
[25]. Mandell JF, Engineering MSU--BDoC and Laboratories SN. DOE/MSU Composite Material Fatigue Database: Test Methods, Materials, and Analysis. Sandia National Laboratories, 1997.
[26]. Mandell JF, Samborsky DD and Cairns D. Fatigue of Composite Materials and Substructures for Wind Turbine Blades. Report no. SAND2002-0771; TRN: US200207%%129 United States 10.2172/793410 TRN: US200207%%129 SNL English, 2002. ; Sandia National Labs., Albuquerque, NM (US); Sandia National Labs., Livermore, CA (US).

[27]. Harris CE. A micromechanics model of the stiffness and strength of laminates with fiber waviness [microform] / Charles E. Harris and Jong-Won Lee. Hampton, Va: National Aeronautics and Space Administration, Langley Research Center, 1988.
[28]. Poe CC, Illg, W., Garber, D. P. Tension Strength of a Thick Graphite/Epoxy Laminate after Impact by a ½-in.-radius Impactor. NASA Technical Memorandum. July 1986 1986. Langley Research Center, Virginia: NASA.
[29]. Poe JCC, B. DH and S. RI. A Review of the NASA Textile Composites Research. 1997. NASA Langley Technical Report Server.
[30]. Kar RJ, Herfert, R.E., Kessler, R.T. Fractographic and Microstructural Examination of Compression Failures in Wet Compression Graphite/Epoxy Coupons. In: Composite Materials: Testing and Design (Seventh Conference) (ed Whitney JM), Philadelphia, PA, 1984, pp.140-157. ASTM International.
[31]. Pottavathri SB, Nair R and Asmatulu R. Effect of In-Plane Fiber Tow Waviness Upon the Tensile Strength Characteristics of Fiber Reinforced Composites of Carbon/Epoxy AS4/3501-6. 2015: V009T012A059. DOI: 10.1115/IMECE2015-52366.
[32]. Raju SK. Shocklam. Wichita, Kansas: Aerospace Engineering Department, Wichita State University, 2015.
[33]. Abaqus. Composites modeling - Documentation Collection. Abaqus CAE user's manual 614. Simulia, 2015.
[34]. Corporation H. 3501-6 Epoxy Matrix Product Data, http://www.hexcel.com/Resources/DataSheets/Prepreg-Data-Sheets/3501-6_eu.pdf (1998, accessed March 12 2016).
[35]. Corporation H. HexTow AS4C Carbon Fiber Product Data, http://www.hexcel.com/resources/datasheets/carbon-fiber-data-sheets/as4c.pdf (2010, accessed March 12 2016).